Desalination and Water Treatment
www.deswater.com
doi: 10.1080/19443994.2014.1003607

57 (2016) 4853–4863
March

Taylor & Francis
Taylor & Francis Group

Geochemical modeling of brine remediation using accelerated carbonation of fly ash

Muriithi Nyambura Grace[a,*], Petrik Felicia Leslie[b], Doucet Jules Frédéric[c]

[a]*Chemistry Department, Maseno University, Private bag, Maseno, Kenya, Tel. +254 722548700; email: gmuriithi@maseno.ac.ke*
[b]*Environmental Nano Sciences Research Group, University of the Western Cape, Private bag X17, Bellville 7535, South Africa, Tel. +27 219593304; email: lpetrik@uwc.ac.za*
[c]*Council for Geoscience, 280 Pretoria Street, Silverton, Private bag X112, Pretoria 0001, South Africa, Tel. +27 0128411300; email: fdoucet@geoscience.org.za*

Received 19 May 2014; Accepted 8 December 2014

ABSTRACT

A protocol is proposed, where waste fly ash and CO_2 emissions from coal-fired power plants are utilized in remediating brine waste. The untreated brine sample was made up of Na^+, SO_4^{2-}, Cl^-, Ca^{2+}, Mg^{2+}, and K^+ as the major ions with trace concentrations of other ions. The brine can thus be classified as $Na_2SO_4^-$-rich water with respect to major cations and anions. Following carbonation, over 99% removal of NO_3^- was achieved while B^{3+}, V^{2+}, MO^{2+}, and Cl^- concentrations increased. Major components removal from brine upon carbonation was as follows: Na^+ (15–29%), Mg^{2+} (53–87%), K^+ (70–88%), Ca^{2+} (40–73%), and SO_4^{2-} (12–36%). Speciation modeling of the major components present in brine showed that Na^+, K^+, and Cl^- exist mainly as free ions, while Mg^{2+} and Ca^{2+} are associated with SO_4^{2-} as well as being in their free forms. SO_4^{2-} ions on the other hand were present in its free form to a great extent as well as associated with Na^+, Ca^{2+}, Mg^{2+}, and K^+, respectively, in a decreasing order. The carbonated brine effluents are therefore depleted with regards to major and trace elements concentration, when compared with the untreated brine. Mineral carbonation may therefore be a potent brine remediation protocol, which can be optimized for maximum removal of various elements.

Keywords: Brine; Mineral carbonation; Fly ash; McNemar test; Geochemical modeling; Speciation

1. Introduction

Saline effluents, also known as brines, are a direct consequence of the drive to save water through desalination. Although much progress into desalination techniques has been made over the past decade, concentrated saline effluents still present a major challenge in finding sustainable treatment and disposal methods [1]. Increasing volumes of domestic, industrial, and agricultural wastes are exerting immense pressure on water resources worldwide. Surface and underground water supplies are not plentiful, especially in countries like South Africa, where the average annual rainfall is half that of the world average [1]. One of the obvious answers to conserve this precious resource is by recycling and reuse of domestic and industrial wastewater. This has led to the production of water suitable for

*Corresponding author.

various applications ranging from irrigation, domestic use, to boiler feed for power generators. Brines generated in industrial applications such as power generation are pollutants, which must be disposed of safely to avoid environmental pollution and to abide by the principles of sustainable development. Since they contain high salt loads, the salts can contaminate underground reservoirs [2]. Having been involved in various projects, investigating fly ash applications in environmental remediation [3,4], specifically in mine water remediation at our research group, it was only valid to try fly ash application in the remediation of brine. This problem is particularly prevalent in power stations, water reclamation plants as well as other industrial outfits. Brine is capable of reacting with CO_2 leading to the formation of carbonates, such as calcite, magnesite, siderite, and dolomite. These carbonates have the capacity to encapsulate major elements from brine to sequester CO_2 and to trap within their matrices trace elements present in brine leading to cleaner brine effluents [2]. This will serve a threefold purpose; clean up of brine wastewaters, waste fly ash utilization, and capture of CO_2 emissions from power stations as mineral carbonates. This study sought to investigate the feasibility of applying fly ash and mineral carbonation in the remediation of waste brine and to subsequently, model the experimental system using the Geochemist's Workbench software package.

2. Experimental

2.1. Sample collection and experimental treatments

Sample collection and mineral carbonation procedure have been reported elsewhere (see Muriithi et al. [5]). In summary, the FA was mixed with brine at different solid to liquid ratios and carbonated at either 30 or 90°C with a pressure of 4 or 1 Mpa as per the experiments designed using the D-optimal statistical design. Carbonation was carried out for 2 h in a high-pressure reactor, after which the solid residues were separated from the leachates and both characterized by various analytical techniques.

2.2. Statistical testing

McNemar's test of significance was carried out to determine the best carbonation factor combinations that were effectual in remediating the brine. Refer to Section 3.3 for further clarification.

2.3. Geochemical modeling

Geochemical modeling was carried to predict the speciation of the brine as well as the mineral formation upon carbonation. Geochemist's Workbench (GWB) Essentials version 8.0 was used in the modeling of the brine using the pH, electrical conductivity (EC), alkalinity, and acidity of the brine, the concentration of individual ions as well as the CO_3^{2-} ions from the CO_2 gas. Concentration of individual ions was carried out using ICP-MS and IC. pH and EC of the brine were measured in the field using a Martini Mi150 portable meter, while alkalinity was determined by acid titration. SpecE8 subprogram of the GWB was used to speciate the raw brine. Possible mineralization was predicted by plotting stability diagrams in the Act2 subprogram of GWB. The independent variable was chosen as pH, while the dependent variable was log activity of the major ions in brine.

3. Results and discussion

3.1. Composition of the untreated brine

The major components identified were SO_4, Na, Cl, Mg, and K. Minor components included Sr, NO_3, Si, Ni, and Pb, while the trace elements comprised of V, B, Ba, Cu, As, Fe, Se, Mn, Mo, Ti, Zn, Cr, Al, and Co (see Table 1).

The composition of the brine was typical of that of $Na_2SO_4^-$-rich waters. Depending on the favorable chemical thermodynamics under the present carbonation experiments, components such as Ca, SO_4, and Mg could be converted into mineral species, such as calcite, gypsum, and magnesite, respectively.

3.2. Effect of carbonation on concentration of various elements present in brine

The effect of carbonation on the raw brine was evaluated by calculating the percentage increase/decrease of various elements after the carbonation process. The following equation was applied.

$$\%\ \text{Increase/decrease} = \frac{\text{Initial concentration} - \text{Final concentration}}{\text{Initial concentration}} \times 100 \quad (1)$$

A table of the corresponding increase or decrease for each element is given in Table 2.

From Table 2, it is clear that carbonation of brine in the presence of fly ash led to the increase in concentration of Cl between 5 and 27% irrespective of the factor combinations (highlighted in bold). The increase is attributable to leaching from fly ash. Fatoba [6] in his chemical analysis of the fly ash obtained from the

Table 1
Major, minor, and trace ion content of untreated brine (ppm; $n = 3$)

Components	Concentration (ppm)
SO_4	11,704 ± 14.28
Na	3,355 ± 25.46
Cl	1,365 ± 7.78
Ca	210.2 ± 10.47
Mg	111.85 ± 0.07
K	78.75 ± 2.05
Sr	11.06 ± 0.18
NO_3	6.5 ± 1.44
Si	2.54 ± 0.03
Ni	2.5 ± 0.02
Pb	1.6 ± 0.01
V	0.4898 ± 0.04
B	0.154 ± 0.01
Ba	0.15 ± 0.01
Cu	0.118
As	0.076 ± 0.01
Fe	0.068 ± 0.02
Se	0.058 ± 0.01
Mn	0.057 ± 0.01
Mo	0.037
Ti	0.029
Zn	0.028
Al	0.023
Cr	0.023
Co	0.020

same power plant as this study, reported Cl concentrations of 730.3 ppm. On the other hand, SO_4, Na, Ca, Mg, and K were reduced in all the experiments conducted as per Table 2 above. The most successful removal rate for SO_4 was observed to be 36%. This run was conducted at 1 Mpa and 30˚C using the <20 μm fraction at a S/L ratio of 0.5. Na and Ca on the other hand had maximum removal of 29 and 73%, respectively, conducted at 4 Mpa and 90˚C at a S/L ratio of 1 using bulk ash. Table 3 summarizes the removal ranges for the major cations.

Table 3 shows that K was removed to the highest degree (between 70 and 88% removal), while Na was removed to the lowest degree (between 15 and 29%). Removal of these major ions from the brine by mineral carbonation goes a long way to simplify it, allowing for downstream recovery of components from brine much easier e.g. by eutectic freeze crystallization [7]. The more complex the brine, the higher the treatment and remediation cost. This protocol, thus allows for reduced cost of elemental recovery downstream. Table 4 gives the percentage removal of trace elements from brine after carbonation.

As seen in Table 4, concentration of B, V, and Mo increased with carbonation irrespective of the factor combinations (highlighted in bold), while 100% removal was achieved for NO_3. V leached between 18 and 234% with carbonation. B and Mo leached into brine to the highest extent with carbonation with maximum values of 2,944 and 14,925%, respectively. It has been reported that B, V, and Mo leach out of fly ash with time [8], due to the formation of oxyanions that are soluble at the pH values of 8–9 attained during the carbonation process [9]. Investigations carried out by Alba et al. [10] on the carbonation of municipal solid waste incineration (MSWI) ash found that carbonation led to elements, such as Pb and Zn co-precipitating with $CaCO_3$, due to the predominance of $PbCO_3$ at pH 6–9 and $Zn(OH)_2$ at pH 9–11. This has been reported elsewhere by [11,12]. Other co-precipitating elements are Cd, Cr, and Cu, and their reduction in the carbonated leachates can be attributed to these co-precipitation reactions.

3.3. Statistical testing using McNemar's test

Statistical analysis (McNemar's test) was then applied to study the best factor combinations for the removal of different elements in brine after carbonation. McNemar's test is also called a test for the significance of change [13]. In the medical field, the test is used to investigate the effect of a medication before and after treatment where the measurements are of the strength of either a nominal or interval scale, for instance, responded or did not respond; improved or did not improve, and positive or negative [14]. McNemar's test [15] was thus chosen as it takes into account paired observations, where in this study, the investigation considered the effect of factor combinations used in the carbonation process and their effect on the concentration of various ions in brine before and after carbonation. Moreover, since there are so many factor combinations and generally only one observation per combination, other types of analyses were found not to be feasible. SAS statistical program (enterprise version) was used to run the test.

Since, it was already discussed that the trend for B, V, Mo, and Cl showed an increase with carbonation or 100% removal in the case of NO_3, these components were left out of the statistical analysis as not much else could be established from their behavior using statistical analysis. Na and SO_4 were removed from brine during carbonation to a maximum of 36% in all the factor combinations applied. However, for Al, Ti, Cr, Mn, Fe, Co, Ni, Cu, Zn, As, Se, Ba, Pb, Si, Sr, Mg, K, and Ca, the percentage removal ranged between 2 and 100% with most values falling below 75%. This

Table 2
Percentage increase/decrease of major components after carbonation

Run No.	Conditions	SO_4	Na	**Cl**	Ca	Mg	K
1	1 Mpa, 90°C, <20 μm, S/L 0.5	25	24	**−27**	58	84	80
2	1 Mpa, 90°C, 20–150 μm, S/L 0.5	23	21	**−13**	45	53	82
3	4 Mpa, 90°C, bulk ash, S/L 0.1	15	20	**−17**	40	69	88
4	1 Mpa, 30°C, <20 μm, S/L 0.5	36	26	**−5**	47	77	81
5	4 Mpa, 90°C, >150 μm, S/L 0.5	20	21	**−21**	55	84	78
6	1 Mpa, 90°C, 20–150 μm, S/L 1	20	24	**−14**	72	63	80
7	1 Mpa, 90°C, >150 μm, S/L 0.1	18	18	**−12**	51	63	70
8	1 Mpa, 30°C, 20–150 μm, S/L 0.1	12	19	**−15**	43	80	86
9	4 Mpa, 90°C, 20–150 μm, S/L 0.1	14	26	**−16**	62	79	80
10	4 Mpa, 30°C, bulk ash, S/L 0.5	16	24	**−12**	53	83	82
11	4 Mpa, 90°C, 20–150 μm, S/L 0.1	14	26	**−18**	43	79	75
12	1 Mpa, 30°C, bulk ash, S/L 0.1	14	17	**−15**	61	87	80
13	4 Mpa, 30°C, 20–150 μm, S/L 1	24	23	**−11**	54	85	85
14	4 Mpa, 90°C, <20 μm, S/L 1	27	24	**−18**	67	81	83
16	1 Mpa, 30°C, bulk ash, S/L 1	25	15	**−6**	49	85	78
17	1 Mpa, 30°C, <20 μm, S/L 0.5	32	21	**−13**	48	83	79
18	1 Mpa, 30°C, <20 μm, S/L 0.1	15	20	**−11**	56	70	86
19	1 Mpa, 30°C, >150 μm, S/L 0.5	16	20	**−9**	65	66	76
20	4 Mpa, 30°C, bulk ash, S/L 1	21	23	**−10**	46	77	74
21	4 Mpa, 90°C, <20 μm, S/L 0.5	34	28	**−13**	54	81	84
22	4 Mpa, 30°C, <20 μm, S/L 1	13	25	**−14**	66	71	81
23	1 Mpa, 30°C, bulk ash, S/L 0.5	28	24	**−11**	51	79	85
24	4 Mpa, 90°C, <20 μm, S/L 0.1	13	25	**−14**	62	83	82
25	4 Mpa, 30°C, >150 μm, S/L 0.1	22	22	**−10**	58	81	79
26	1 Mpa, 90°C, 20–150 μm, S/L 0.1	15	23	**−15**	55	64	81
27	1 Mpa, 90°C, bulk ash, S/L 0.5	19	21	**−18**	56	70	87
28	4 Mpa, 30°C, 20–150 μm, S/L 0.5	24	21	**−15**	49	79	77
29	1 Mpa, 30°C, >150 μm, S/L 0.1	14	22	**−13**	53	83	84
31	4 Mpa, 90°C, bulk ash, S/L 1	21	29	**−8**	73	72	83

Note: The +ve values indicate decrease, while –ve values indicate increase with carbonation.

Table 3
Major components removal range

Component	% Removal range
SO_4	12–36
Na	15–29
Ca	40–73
Mg	53–87
K	70–88

formed the basis for setting the threshold restrictions to be applied in the statistical analysis. A cut-off threshold of 70% for Al, Ti, Cr, Mn, Fe, Co, Ni, Cu, Zn, As, Se, Ba, Pb, Si, Sr, Mg, K, and Ca was chosen, while for Na and SO_4 a cut-off threshold of 20% was chosen. This was informed by the high frequencies for these two values for the respective elements, in order to consider the removal process successful, if the reduction was met or exceeded the given cut-off thresholds. The proportion of times the process was a success was evaluated over the 20 measured components (after removing B, V, Mo, Cl, and NO_3 as stated previously). The evaluation was made relative to the combination of factors used (i.e. temperature, particle size, pressure, and S/L ratio). In running the test, successful removal was set as 1 (i.e. when the set threshold was attained), while a failure was set as 0 (i.e. the set threshold was not attained). Table 5 gives the statistical output using SAS statistical software.

As can be seen from Table 5, there was one combination that was successful in all 20 cases (i.e. gave 100% removal) and one that was successful in 18/20 = 90% of the cases. The poorest combination was only successful in 9/20 = 45% of the cases. The null hypothesis was set to state that there is a difference in the percentage removal of elements with application of various treatment conditions. On the other hand, the

Table 4
Percentage increase/decrease of minor and trace components after carbonation

Run No.	Conditions	Sr	NO_3	Si	Ni	Pb	**V**	**B**	Ba	Cu	As	Fe	Se	Mn	**Mo**	Ti	Zn	Al	Cr	Co
1	1 Mpa, 90˚C, <20 μm, S/L 0.5	91	100	90	54	92	**−141**	**−1,234**	20	41	40	85	100	84	**−10,738**	100	63	13	81	97
2	1 Mpa, 90˚C, 20–150 μm, S/L 0.5	97	100	99	83	55	**−52**	**−2,326**	75	94	54	66	80	90	**−5,799**	76	91	100	64	99
3	4 Mpa, 90˚C, bulk ash, S/L 0.1	82	100	94	75	54	**−217**	**−1,125**	64	99	8	68	72	62	**−1,539**	89	85	7	78	99
4	1 Mpa, 30˚C, <20 μm, S/L 0.5	95	100	99	94	42	**−35**	**−1,056**	21	87	6	81	92	98	**−7,884**	60	86	39	42	91
5	4 Mpa, 90˚C, >150 μm, S/L 0.5	97	100	82	63	88	**−104**	**−1905**	42	28	40	68	86	65	**−3,086**	65	77	6	19	89
6	1 Mpa, 90˚C, 20–150 μm, S/L 1	98	100	87	80	92	**−190**	**−893**	15	90	81	78	100	45	**−11,407**	8	96	28	51	97
7	1 Mpa, 90˚C, >150 μm, S/L 0.1	97	100	92	72	69	**−191**	**−476**	67	100	61	64	46	75	**−1,011**	77	76	31	69	99
8	1 Mpa, 30˚C, 20–150 μm, S/L 0.1	86	100	87	71	75	**−49**	**−790**	23	78	76	79	100	95	**−1,076**	43	73	7	79	90
9	4 Mpa, 90˚C, 20–150 μm, S/L 0.1	91	100	89	72	70	**−129**	**−1,175**	70	94	90	90	100	66	**−1,295**	85	76	100	80	98
10	4 Mpa, 30˚C, bulk ash, S/L 0.5	90	100	100	58	76	**−105**	**−2,552**	46	88	34	87	92	83	**−4,893**	38	41	100	48	95
11	4 Mpa, 90˚C, 20–150 μm, S/L 0.1	97	100	93	73	43	**−137**	**−1,268**	81	96	91	67	100	69	**−1,478**	78	49	41	44	98
12	1 Mpa, 30˚C, bulk ash, S/L 0.1	95	100	86	96	100	**−85**	**−896**	28	96	66	77	100	91	**−1,241**	74	63	55	81	90
13	4 Mpa, 30˚C, 20–150 μm, S/L 1	85	100	70	81	86	**−65**	**−1817**	59	94	67	80	100	94	**−6,650**	74	58	100	38	99
14	4 Mpa, 90˚C, <20 μm, S/L 1	96	100	95	72	79	**−32**	**−943**	80	56	76	73	100	82	**−14,925**	61	2	47	77	96
16	1 Mpa, 30˚C, bulk ash, S/L 1	94	100	96	87	67	**−69**	**−540**	92	95	81	72	65	100	**−3,553**	71	77	37	83	100
17	1 Mpa, 30˚C, <20 μm, S/L 0.5	91	100	87	43	85	**−137**	**−2,944**	53	32	18	45	100	84	**−5,680**	42	80	42	57	81
18	1 Mpa, 30˚C, <20 μm, S/L 0.1	93	100	84	47	92	**−49**	**−1,718**	86	40	37	88	63	84	**−2066**	96	59	33	26	77
19	1 Mpa, 30˚C, >150 μm, S/L 0.5	43	100	93	86	82	**−41**	**−1,032**	21	93	85	67	80	94	**−1816**	53	62	36	43	95
20	4 Mpa, 30˚C, bulk ash, S/L 1	92	100	91	90	91	**−181**	**−921**	55	100	74	79	52	100	**−4,514**	93	89	48	82	100
21	4 Mpa, 90˚C, <20 μm, S/L 0.5	95	100	98	78	85	**−30**	**−1858**	73	75	87	68	60	53	**−8,600**	23	85	19	77	97
22	4 Mpa, 30˚C, <20 μm, S/L 1	93	100	78	59	78	**−149**	**−2,646**	53	76	100	76	100	83	**−13,612**	59	59	14	68	91
23	1Mpa, 30˚C, bulk ash, S/L 0.5	85	100	94	83	87	**−37**	**−464**	91	100	91	88	100	100	**−2,949**	94	63	100	83	100
24	4 Mpa, 90˚C, <20 μm, S/L 0.1	94	100	92	63	96	**−179**	**−2,412**	54	86	55	50	100	74	**−5,996**	77	69	42	87	94
25	4 Mpa, 30˚C, >150 μm, S/L 0.1	98	100	94	67	100	**−85**	**−1867**	68	91	87	89	100	91	**−2,113**	85	66	38	72	98
26	1 Mpa, 90˚C, 20–150 μm, S/L 0.1	91	100	87	46	97	**−24**	**−363**	31	90	84	71	100	79	**−740**	69	36	38	100	79
27	1 Mpa, 90˚C, bulk ash, S/L 0.5	78	100	62	63	100	**−234**	**−886**	84	100	65	87	100	41	**−1880**	95	86	100	95	100
28	4 Mpa, 30˚C, 20–150 μm, S/L 0.5	83	100	97	81	93	**−55**	**−3,049**	80	100	77	81	100	84	**−5,306**	41	53	100	17	98
29	1 Mpa, 30˚C, >150 μm, S/L 0.1	94	100	95	96	87	**−38**	**−465**	18	90	98	91	100	80	**−786**	80	75	16	38	85
31	4 Mpa, 90˚C, bulk ash, S/L 1	99	100	100	100	100	**−18**	**−802**	74	100	100	100	100	100	**−221**	100	100	100	98	97

Notes: The +ve values indicate decrease,
while –ve values indicate increase with carbonation.

Table 5
SAS output on the classification of the various runs according to the set thresholds with at least 70% element removal (or 20% element removal)

Observation	Run	Carbonation conditions	Percentage removal
1	31	4 Mpa, 90℃, bulk ash, S/L 1	100
2	23	1 Mpa, 30℃, bulk ash, S/L 0.5	90
3	9	4 Mpa, 90℃, 20–150 μm, S/L 0.1	85
4	20	4 Mpa, 30℃, bulk ash, S/L 1	80
5	28	4 Mpa, 30℃, 20–150 μm, S/L 0.5	80
6	16	1 Mpa, 30℃, bulk ash, S/L 1	75
7	29	1 Mpa, 30℃, >150 μm, S/L 0.1	75
8	13	4 Mpa, 30℃, 20–150 μm, S/L 1	75
9	14	4 Mpa, 90℃, <20 μm, S/L 1	75
10	25	4 Mpa, 30℃, >150 μm, S/L 0.1	75
11	8	1 Mpa, 30℃, 20–150 μm, S/L 0.1	70
12	27	1 Mpa, 90℃, bulk ash, S/L 0.5	70
13	2	1 Mpa, 90℃, 20–150 μm, S/L 0.5	70
14	6	1 Mpa, 90℃, 20–150 μm, S/L 1	70
15	21	4 Mpa, 90℃, <20 μm, S/L 0.5	70
16	12	1 Mpa, 30℃, bulk ash, S/L 0.1	65
17	1	1 Mpa, 90℃, <20 μm, S/L 0.5	65
18	4	1 Mpa, 30℃, <20 μm, S/L 0.5	65
19	10	4 Mpa, 30℃, bulk ash, S/L 0.5	*60*
20	11	4 Mpa, 90℃, 20–150 μm, S/L 0.1	*60*
21	22	4 Mpa, 30℃, <20 μm, S/L 1	*60*
22	24	4 Mpa, 90℃, <20 μm, S/L 0.1	*60*
23	26	1 Mpa, 90℃, 20–150 μm, S/L 0.1	*60*
24	3	4 Mpa, 90℃, bulk ash, S/L 0.1	*55*
25	18	1 Mpa, 30℃, <20 μm, S/L 0.1	*55*
26	17	1 Mpa, 30℃, <20 μm, S/L 0.5	*55*
27	19	1 Mpa, 30℃, >150 μm, S/L 0.5	*50*
28	5	4 Mpa, 90℃, >150 μm, S/L 0.5	*50*
29	7	1 Mpa, 90℃, >150 μm, S/L 0.1	*45*

alternative hypothesis was set to state that there is no difference in the percentage elemental removal with application of varying treatment conditions. The null hypothesis is usually rejected, when the calculated p value is less than the set p value of 0.01 and accepted, when the calculated p value is greater than the set p value of 0.01. Since, there were many pairs of combinations that could be considered ($N \times N/2 \approx 351$ possible pairwise combinations), the p value was adjusted for multiple testing and used at 0.01 level of significance rather than the normal 0.05, thus a 99% confidence interval instead of the usual 95% confidence interval. With these more stringent conditions, it can be seen, the conditions applied in run 31 (100% successful) was more significant in cleaning the brine of undesirable components. On the other hand, run 7 (45%) at 1 Mpa and 90℃ using the >150 μm particle fraction at a S/L ratio of 0.1 was significantly lower than run 31 (100%), and run 23 (90%) with the p-value in the latter case being 0.0117. Comparisons of runs 4 and 17 are also shown as these experiments used the same levels of all factors. The differences in percentage removal of the elements of interest observed for these runs are not statistically significant, but do indicate some variability from one run to the next (even with the same levels of factors i.e. runs 4 and 17 were at 1 Mpa, 30℃, <20 μm, and S/L ratio of 0.5). This could be attributed to the inhomogeneity of the fly ash used in the carbonation process, where the CaO content of each carbonation experiment cannot be accurately ascertained. The highlighted in italic part (Table 5) shows the observations, for which the outcome was significantly different from the 100% removal (run 31). At the top or bottom of the table, not much significant difference was observed for instance run 5 and run 7 are not statistically significantly different from each other. A pairwise comparison was carried out for various runs 7 and 23 as given in Table 6 below.

From the frequency Table 6 above, run 23 had a success rate of 90% with 18 observations being

Table 6
Pairwise comparison for Runs 7 and 23 using SAS

```
c
o
n                    p
d                    c
i                    t
t                    _
i                    g
O   R                 o                    o                              x  xxxxxxxxxxxxxxx
b   u                 n                    o   x  xxxxxxxx  1  1  1  1  1  1  1  1  1  2  2  2  2  2  2
s   n                 s                    d   1  2  3  4  5  6  7  8  9  0  1  2  3  4  5  6  7  8  9  0  1  2  3  4  5

1  23  1Mpa, 30 ºC, bulk ash, S/L 0.5  0.90  1  1  1  1  1  1  1  1  0  1  1  1  1  1  1  .  .  .  .  1  1  0  1  .  1
2   7  1Mpa, 90 ºC, >150 µm, S/L 0.1   0.45  0  1  0  1  0  1  1  1  1  0  0  0  0  1  1  .  .  .  .  0  1  0  0  .  0

Pairwise comparison for runs 7 and 23
The FREQ Procedure
Table of run7 by run23

run7      run23

Frequency|
Percent  |       0|       1|  Total
---------+--------+--------+
       0 |      1 |     10 |     11
         |   5.00 |  50.00 |  55.00
---------+--------+--------+
       1 |      1 |      8 |      9
         |   5.00 |  40.00 |  45.00
---------+--------+--------+
Total           2       18       20
           10.00    90.00   100.00

Frequency Missing = 5

McNemar's Test
Statistic (S)         7.3636
DF                         1
Asymptotic Pr>  S     0.0067
Exact      Pr>= S     0.0117
```

positive and 2 observations being negative (the set threshold of removal was achieved up to 90%), while run 7 only achieved 45% success with 9 positive observations and 11 negative observations. The *p*-value of 0.0117 obtained shows the two runs are significantly different considering the confidence interval chosen of 0.01. The missing frequency is the five elements removed in the analysis (B, V, Mo, Cl, and NO_3 as explained before).

3.4. Geochemical modeling using Geochemist Workbench software

3.4.1. Physicochemical speciation of the brine

Speciation of the brine solution allows for prediction of the association of major cations and anions in the brine. For this analysis, only the major ions from ICP-MS and IC analysis as given in Table 1 are presented in the geochemical modeling. These ions are SO_4^{2-}, Cl^-, Na^+, Ca^{2+}, Mg^{2+}, and K^+. According to McLean and Bledsoe [16], metals exist in solution either as free ions, in various soluble complexes with inorganic or organic ligands or associated with mobile inorganic and organic colloidal materials. Speciation not only affects the mobility of metals, but also the bioavailability and toxicity of the metal. Free metal ions are the most bioavailable and toxic form of the metal. Fig. 1 gives the speciation of Na^+ and K^+ in the brine solution.

Modeling predicted that Na^+ in the brine would occur mostly as free Na^+ ions, while a small amount would be associated with the SO_4^{2-} ions. Additionally, Na^+ may also occur in association with other species such as, HCO_3^-, Cl^-, HPO_4^-, and CO_3^{2-} in trace concentrations. Speciation of K^+ in brine is only expected

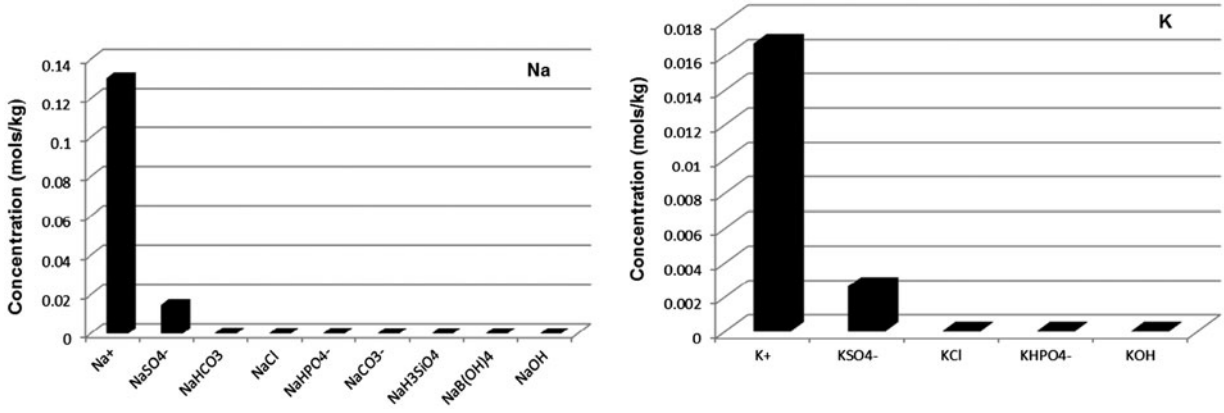

Fig. 1. Speciation of Na^+ and kin brine.

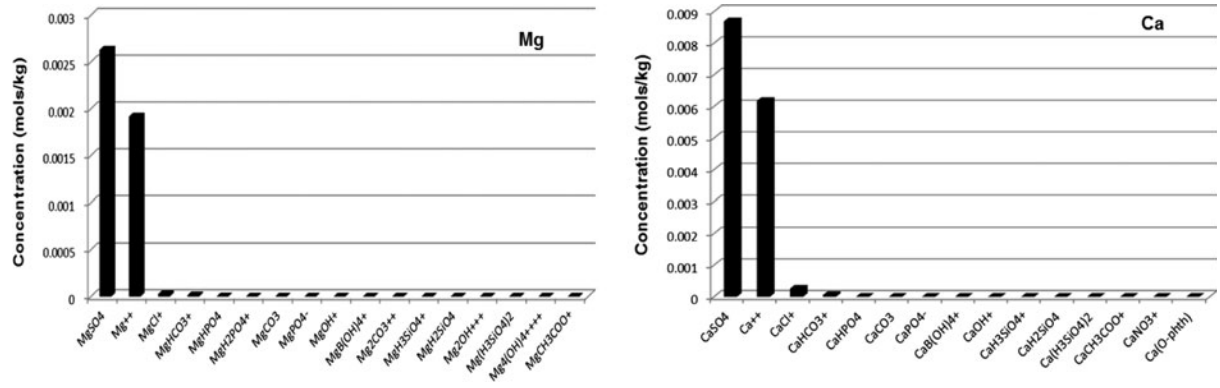

Fig. 2. Mg^{2+} and Ca^{2+} speciation in brine.

with a few anions, such as SO_4^{2-}, Cl^-, HPO_4^-, and OH^-, while most of the K^+ would exist in its free ionic form in the brine.

Fig. 2 shows the speciation of Mg^{2+} and Ca^{2+}.

The speciation of $Mg^{2+}$and Ca^{2+} were predicted to be almost the same, in the sense that the main forms of these elements would be found in association with SO_4^{2-} or as the free cations in the brine. A very small

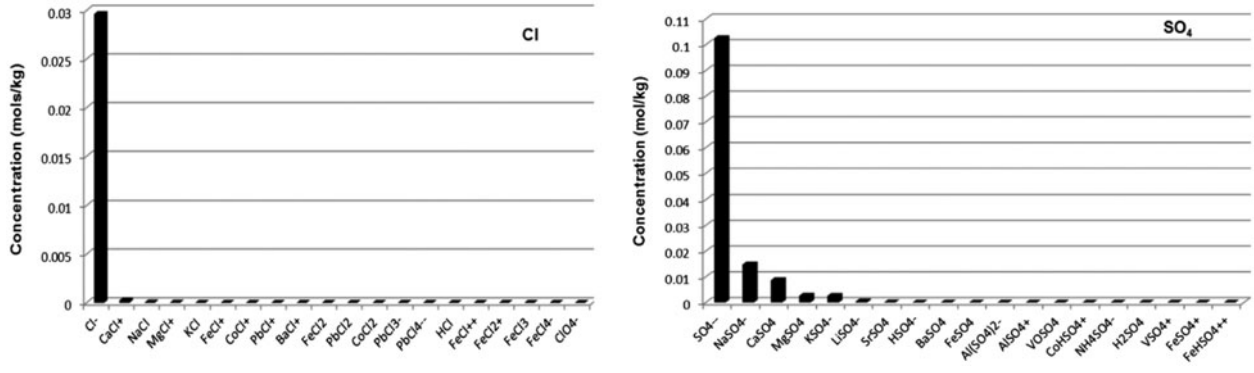

Fig. 3. Cl^- and SO_4^{2-} speciation in brine.

proportion of these two cations could be found in association with the Cl^- and HCO_3^- ions in the brine. $Cl^-$and SO_4^{2-} speciation is given in Fig. 3 below.

Fig. 3 shows that speciation of Cl^- in brine was predicted to be largely controlled by the free Cl^- ions. The other ionic species may exist in negligible concentrations, although it is important to note that these other species may also be formed. Most of the SO_4^{2-} in brine is predicted to occur in the free form, although some possible association with Na^+, Ca^{2+}, Mg^{2+}, and K^+ was also noted.

3.4.2. Stability diagrams

Stability diagrams are used as a convenient technique for illustrating how the solubility of metal compounds varies with pH and with metal concentration [16]. Figs. 4 and 5 show the stability diagrams for the main ions in brine (i.e. Ca^{2+}, Mg^{2+}, Na^+, K^+, Cl^-, and SO_4^{2-}). Stability of each ion is established in the presence of other major ions in order to probe the associations possible in the brine solution. Red lines represent equilibrium conditions between the mineral forms and the aqueous species. Both solid and ionic species are observed in the stability diagrams in Figs. 4 and 5.

Stability of Ca (Fig. 4(a)) was affected by both the activity and the pH. Ionic species observed are Ca^{2+}, $CaSO_4$, and $Ca(OH)_2$, while predicted precipitated minerals were gypsum, dolomite, and calcite. Dolomite and calcite precipitation was predicted to occur in alkaline pH, while gypsum precipitation, which seems to be affected mostly by activity rather than pH was predicted between acidic and neutral pH values.

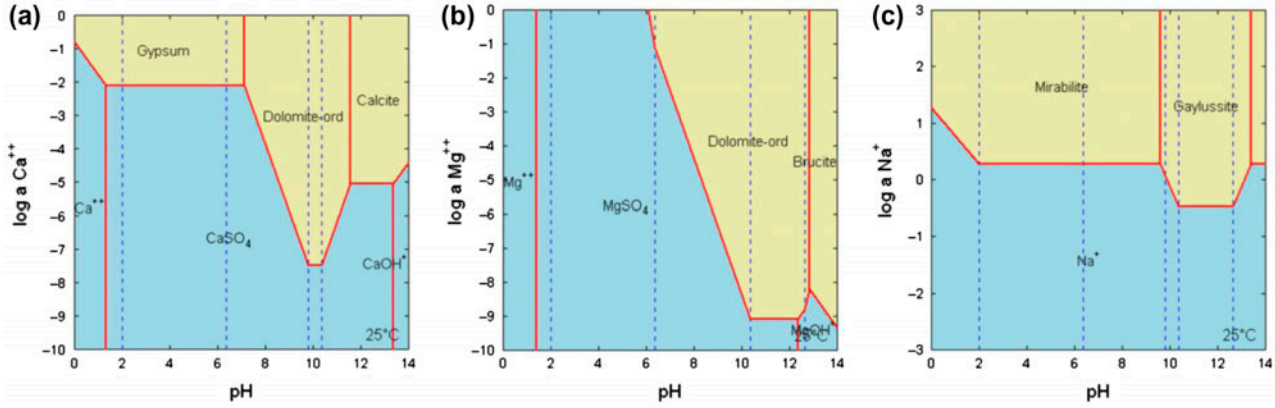

Fig. 4. Stability diagrams for Ca^{2+} (a), Mg^{2+} (b), and Na^+ (c) (blue section represents the ionic species, while yellow represents the mineral phases).

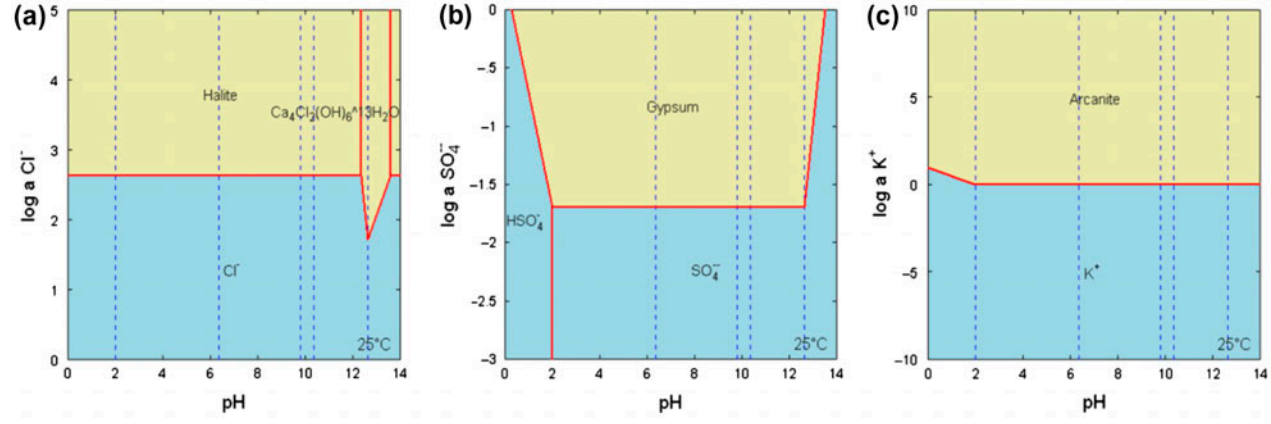

Fig. 5. Stability diagrams for Cl^- (a), SO_4^{2-} (b), and K^+ (c) (blue section represents the ionic species, while yellow represents the mineral phases).

In the case of Mg^{2+}, at acidic to neutral pH values, the ionic species of Mg^{2+} and $MgSO_4$ dominated in solution (Fig. 4(b)). However, as the pH rose to alkaline values, precipitation of ordered dolomite and brucite was predicted. It can thus be concluded that at low pH values, in spite of the relative concentration of the Mg^{2+} ions, no precipitation would occur. Stability of Mg is thus a function of both activity and pH.

The stability of Na^+ ions in the brine is a function of activity only and is not pH dependent (Fig. 4(c)). This was evidenced by the fact that precipitation of mirabilite ($Na_2SO_4{\cdot}10H_2O$) and gaylussite ($Na_2Ca(CO_3)_2{\cdot}5H_2O$) (the two possible mineral phases) was predicted to occur only at an activity above zero, below which only Na^+ ions are available in the brine solution. Mirabilite is predicted to form at a salinity of 100 g/l. Na^+ is a conservative ion and will not easily precipitate as a solid, thus remaining in solution.

Stability of Cl^- is activity dependent, as it was predicted that below the activity of 3, irrespective of the pH, Cl^- exists as the free ion (Fig. 5(a)). However, from around activity of 3, precipitation is possible with the formation of halite (NaCl) and $Ca_4Cl_2(OH)_6{\cdot}13H_2O$. From Table 1, the concentration of Cl in brine was 1,365 ppm, while that of Na was 3,355 ppm. Cl is thus the limiting reagent in the precipitation of halite, hence, the observed predicted precipitation of halite in the solubility diagram for Cl (Fig. 5(a)) and not in the stability diagram for Na (Fig. 4(c)).

Fig. 5(b) shows that the stability of SO_4^{2-} is both activity and pH dependent. At pH values below 2, SO_4^{2-} ions are predicted to be present in solution as the bisulfate (HSO_4^-) form. Between pH 2 and 13 with an activity of −1.5, the formation of gypsum would be the predominant process. In the same pH range, below activity of −1.5, SO_4^{2-}ions are predicted to be present in the free form in the brine solution.

Fig. 5(c) shows that K^+ solubility is activity dependent only and that below zero activity, K^+ is predicted to exist in the free form in the brine solution, in spite of the pH value. Above zero activity, precipitation with SO_4^{2-} is possible leading to the formation of arcanite (K_2SO_4). This prediction is supported by the speciation diagram (Fig. 1), where the majority of the K^+ was observed to occur in free form.

The carbonated brine elemental concentration was input into the GWB software to predict the possible mineral phases expected to form with carbonation. Run 31, which had been observed to have the highest percentage removal of the elements in brine from statistical analysis was used. Only minerals that were supersaturated in the carbonation leachates (positive saturation indices indicating precipitation) are presented, while the undersaturated minerals (negative saturation indices) are neglected as they are not predicted to precipitate during carbonation. The saturation indices calculated are given in Table 7.

Table 7
Saturation indices of the mineral phases possible during carbonation

Mineral	Formula	Mineral saturation indices
Dolomite-ord	$(CaMg)(CO_3)_2$	2.4088
Witherite	$BaCO_3$	1.0776
Dolomite-dis	$(CaMg)(CO_3)_2$	0.8644
Calcite	$CaCO_3$	0.6458
Aragonite	$CaCO_3$	0.4809
Strontianite	$SrCO_3$	0.1703
Magnesite	$MgCO_3$	0.1341

Notes: Only phases which were supersaturated are shown.

From Table 7 the carbonate forms that are possible with carbonation of brine and fly ash were predicted to be dolomite, witherite, calcite, aragonite, strontainite, and magnesite. Competitive adsorption of elements, such as Ba and Sr was observed while magnesite, calcite, aragonite, and dolomite were the main carbonate forms expected to precipitate. In the carbonation of steel slag by Huijgen [17], Ba and S concentrations in the leachate were observed to follow the witherite and strontianite solubility curves at pH ≥ 8.

4. Conclusions

Raw brine is made up of Na, SO_4, Cl, Ca, Mg, and K as the major ions with trace concentration of other ions. The waters can thus be classified as Na_2SO_4 with respect to major cations and anions. With carbonation, over 99% removal of NO_3 was obtained while B, V, Mo, and Cl concentrations increased. B has been known to leach from FA; moreover, B, V, and Mo are known to form oxyanions that are soluble at alkaline pH levels attained during carbonation. Major components removal from brine with carbonation was as follows: Na (15–29%), Mg (53–87%), K (70–88%), Ca (40–73%), and SO_4 (12–36%). On the other hand, the removal ranges for trace elements was as follows: Sr (43–99%), NO_3 (over 99% removal for all the experimental runs), Si (62—over 99%), Ni (43—over 99%), Pb (42—over 99%), Ba (15–86%), Cu (28—over 99%), As (6—over 99%), Fe (45—over 99%), Se (46—over 99%), Mn (41—over 99%), Ti (8—over 99%), Zn (2—over 99%), Al (7—over 99%), Cr (17—over 99%), and Co (77—over 99%). McNemar's statistical testing showed that Run 31 at 4 Mpa, 90˚C, using bulk ash at

a S/L ratio of 1 had the best factor combination with an element reduction rate of 100% upon carbonation. Speciation modeling of the major elements present in brine showed that Na^+, K^+, and Cl^- exist mainly as free ions, while Mg^{2+} and Ca^{2+} are associated with SO_4^{2-} as well as in their free forms. SO_4^{2-} ions on the other hand were present in free form to a great extent as well as associated with Na^+, Ca^{2+}, Mg^{2+}, and K^+, respectively, in a reducing order. Stability diagrams plotted for the major ions showed the possible mineral forms that may precipitate upon carbonation. Ca^{2+} precipitation and mineral formation is associated with gypsum, dolomite, and calcite. Mg^{2+} is associated with both dolomite and brucite formation. Na^+ could precipitate as mirabilite and gaylussite, while Cl^- is mainly associated with halite and to a lesser extent $Ca_4Cl_2(OH)_6{\cdot}13H_2O$. SO_4^{2-} ions are only capable of precipitating in the form of gypsum, while K^+ is associated with arcanite. Saturation indices showed that the carbonation leachates were supersaturated with respect to dolomite (both ordered and disordered), witherite, calcite, aragonite, strontianite, and magnesite. However, thermodynamics favors the precipitation of calcite, and hence its nucleation and subsequent precipitation is faster than for the other minerals.

Acknowledgments

This research was financially supported by the NRF and the Water Research Commission (WRC) Project Number: K5/ 2,128.

References

[1] A. Nyamhingura, Characterization and Chemical Speciation Modelling of Saline Effluents at Sasol Synthetic Fuels Complex-Secunda and Tutuka Power Stations, MSc Dissertation, University of the Western Cape, South Africa, 2010.

[2] G.N. Muriithi, W.M. Gitari, L.F. Petrik P.G. Ndung'u, Carbonation of brine impacted fractionated coal fly ash: Implications for CO_2 sequestration, J. Environ. Manage. 92 (2011) 655–664.

[3] G. Madzivire, W.M. Gitari, T.V. Ojumu, G. Balfour, N. Misheer L.F. Petrik, Removal of sulphates from South African mine water using coal fly ash, IMWA2010, Pretoria.

[4] W.M. Gitari, L.F. Petrik, O. Etchebers, D.L. Key, E. Iwuoha, C. Okujeni, Passive neutralization of acid mine drainage by fly ash and its derivatives: A column leaching study, Fuel 87 (2008) 1637–1650.

[5] G.N. Muriithi, L.F. Petrik, O.O. Fatoba, W.M. Gitari, F.J. Doucet, J. Nel, S.M. Nyale, P.E. Chuks, Comparison of CO_2 capture by *ex-situ* accelerated carbonation and in *in-situ* naturally weathered coal fly ash, J. Environ. Manage. 127 (2013) 212–220.

[6] O.O. Fatoba, Chemical Interactions and Mobility of Species in Fly Ash Brine Co-disposal Systems, PhD Dissertation, University of the Western Cape, South Africa, 2011.

[7] D.G. Randall, J. Nathoo, A.E. Lewis, A case study for treating a reverse osmosis brine using eutectic freeze crystallization—Approaching a zero waste process, Desalination 266 (2011) 256–262.

[8] J. Jankowski, R.C. Ward, D. French, S. Grores, Mobility of trace elements from selected Australian fly ash and its potential on aquatic ecosystems, Fuel 85 (2006) 234–256.

[9] A.G. Kim, P. Hesbach, Comparison of fly ash leaching methods, Fuel 88 (2009) 926–937.

[10] N. Alba, E. Vazquez, S. Gasso, M.J. Baldasano, Stabilization/solidification of MSW incineration residues from facilities with different air pollution control systems: Durability of matrices versus carbonation, Waste Manage. 21 (2001) 313–323.

[11] H. Ecke, Sequestration of metals in carbonated municipal solid waste incineration (MSWI) fly ash, Waste Manage. 23 (2003) 631–640.

[12] H. Ecke, N. Menadand, A. Lagerkvist, Treatment oriented characterization of dry scrubber residue from municipal solid waste (MSWI), J. Mater. Cycles and Waste Manage. 4 (2002) 117–126.

[13] B.D. Saunders, R.G. Trapp, Basic and Clinical Biostatistics, second ed., Appleton and Lange, Connecticut, CT, 1994.

[14] R.F. Mould, Introductory Medical Statistics, third ed., Institute of Physics Publishing, Bristol, 1998.

[15] Q. McNemar, Note on the sampling error of the difference between correlated proportions or percentages, Psychometrika 12 (1974) 153–157.

[16] J.E. McLean, B.E. Bledsoe, Behavior of Metals in Soils, Ground Water Issue. U.S. EPA, Washington, DC, 1992.

[17] J.J.W. Huijgen, Carbon dioxide Sequestration by Mineral Carbonation, PhD Dissertation, Energy Research Centre of the Netherlands, Petten, 2006, ISBN: 90-8504-573-8.